ISSN 2176-5480

22nd International Congress of Mechanical Engineering (COBEM 2013)
November 3-7, 2013, Ribeirão Preto, SP, Brazil

SIMULATION OF THE SUPERELASTIC BEHAVIOR OF NI-TI SMA BELLEVILLE WASHERS USING ANSYS®

Paulo César Sales da Silva
Universidade Federal de Campina Grande (UFCG), Campina Grande – PB, Brazil
paulocesarsales@outlook.com
Carlos José de Araújo
Universidade Federal de Campina Grande (UFCG), Campina Grande – PB, Brazil
carlos@dem.ufcg.edu.br
Marcelo Amorim Savi
Universidade Federal do Rio de Janeiro (UFRJ), Rio de Janeiro – RJ, Brazil
savi@ufrj.br
Neilor César Santos
Instituto Federal da Paraíba (IFPB), João Pessoa – PB, Brazil
neilor@ifpb.edu.br

Abstract. *Shape memory alloys (SMAs) are capable of recovering large strains after a proper heating and/or mechanical loading process. Several applications are exploiting this remarkable property and Belleville washers are of special interest to perform connections in different industrial situations. This work aims to perform numerical simulations of the superelastic behavior of NiTi SMA Belleville washers. Finite element method is employed making use of commercial software ANSYS Mechanical APDL 14.5. Axisymmetric flat elements are empployed. Characteristic responses of the device are analyzed by considering force-displacement curves assuming different geometrical configurations characterized by dimensionless parameters such as the height/thickness ratio and outer/inner radius ratio. Besides geometrical configurations, temperature influence is investigated. Numerical simulations show aspects of the superelastic recovery, which is also a function of temperature, and it should be highlighted the "duckbill" behavior observed in the force-displacement curves.*

Keywords: *Simulation, Superelasticity, Finite Element Method, Belleville Washers, ANSYS.*

1. INTRODUCTION

Shape Memory Alloys (SMAs) belong to a special group classified as smart or intelligent materials, responding mechanically to non-mechanical stimuli such as temperature and magnetic fields. SMA has the ability to recover large pseudo plastic strains (up to 8%) by a simple heating to a critical temperature characteristic of each alloy. This level of strain recovering is high compared to the one of conventional materials which present elastic strain recovers, of the order of 0.2%. Among the smart materials most frequently used, the SMA are those with the highest energy densities of action, i.e., are able to recover large strains even subjected to large mechanical loading (Lagoudas, 2008).

The active behavior of SMA is due to the crystallographic reversible martensitic phase transformation that occurs in the solid state. This thermoelastic martensitic transformation is responsible for two main thermomechanical characteristics of SMAs: the shape memory effect (SME) and superelasticity (SE) (Otsuka & Wayman, 1998). The first effect is activated by a temperature change when the SMA is deformed in the martensitic state (low temperature phase and lower stiffness) and is then heated to the austenitic phase (high temperature phase and higher stiffness) recovering fully the original shape (martensitic state). On the other hand, the superelasticity or pseudoelasticity occurs when working with SMA above the temperature A_f, characteristic from which the entire crystallographic structure is austenitic. When the SMA is at this state, mechanical loading and unloading is enough to obtain the full recovery of the imposed strain, requiring no heating.

SMA actuators with conical shape, as Belleville washers, may be able to recover pre-loads that may be reduced due to a possible relaxation of a bolt connection due to exposure to high operating temperatures (between 50°C and 150°C) and mechanical vibrations. Moreover, other potential advantage related to the use of Belleville SMA washer would be the stiffness increase of the bolted connection after shape recovery and continued rise in the temperature to above the final transformation temperature of the SMA. This activated state of the SMA actuator can provide large strains under an almost constant loading in the bolted connection due to the phenomenon of superelasticity. Under this condition, the device does not present loss of the pre-load, which would not be possible in a conventional bolted connection using common washers and bolts. Therefore, this smart actuator may have a tapered bifunctional behavior of force generation associated with increased stiffness and superelasticity, dependent only on the temperature of the application. It is noteworthy that there are very few studies in the international literature related to SMA conical Belleville washers, most of them being experimental studies (Labrecque *et al*, 1996; Speicher *et al*, 2009; Speicher, 2010; Pereira *et al*, 2011; Simões, 2012).

This work deals with numerical simulations of the superelastic behavior of SMA conical Belleville washers via finite element method (FEM). The commercial software ***ANSYS Mechanical APDL 14.5*** (ANSYS, 2013) is employed. It is analyzed the characteristic response of force-displacement curves varying geometrical aspects represented by dimensionless parameters such as height/thickness (*h/t*) and outer/inner radius (R_e/R_i) of the SMA Belleville actuator as a function of temperature. Results show a phenomenon called "duckbill" characterized by a hysteretic behavior of the force-displacement curve.

2. METHODOLOGY

2.1 SMA model for superelasticity

There are several ways to describe the thermomechanical behavior of SMAs. Lagoudas (2008) presented a general overview related to the constitutive description of SMAs. ANSYS® software describes the superelastic behavior of SMA actuators by considering a constitutive model proposed by Auricchio *et al.* (1997, 2001).

This model considers two phases: austenite (A) and stress-induced martensite (S). In this regard, the phase-transformation mechanisms involved in superelastic behavior is describe in a macroscopic point of view as follows: austenite to stress-induced martensite (A – S) and stress induced martensite to austenite (S – A). Two internal variables are defined considering martensite volume fraction (β_S) and austenite volume fraction (β_A). These variables have restrictions related to phase coexistence and therefore it is possible to consider only one independent variable:

$$\beta = \beta_S = 1 - \beta_A \tag{1}$$

The material behavior is assumed to be isotropic. The pressure dependence of the phase transformation is modeled by introducing the Drucker-Prager loading function, as established from Eqs. (2) to (5):

$$F = q + 3\alpha p \tag{2}$$

$$q = \sqrt{\frac{3}{2}\mathbf{S}:\mathbf{S}} \tag{3}$$

$$\mathbf{S} = \sigma - \mathbf{p}1 \tag{4}$$

$$p = \frac{1}{3}\sigma:\mathbf{1} \tag{5}$$

where α is a material parameter, σ is the stress, and **1** is the identity tensor.

The evolution of the martensitic volume fraction, $\dot{\beta}_S$ is then defined as follows in Eq. (6):

$$\dot{\beta} = \dot{\beta}_S = \begin{cases} -\mathrm{H}^{AS}(1-\beta)\frac{\dot{F}}{F-{R_f}^{AS}} & \mathrm{A} \rightarrow \mathrm{S\ transformation} \\ \mathrm{H}^{SA}(\beta)\frac{\dot{F}}{F-{R_f}^{SA}} & \mathrm{S} \rightarrow \mathrm{A\ transformation} \end{cases} \tag{6}$$

where ${R_f}^{AS} = {\sigma_f}^{AS}(1+\alpha)$ and ${R_f}^{SA} = {\sigma_f}^{SA}(1+\alpha)$.

Besides, ${\sigma_f}^{AS}$ and ${\sigma_f}^{SA}$ are critical stress parameters defined in Fig. (1). The H parameters are defined as follows by Eqs. (7) and (8):

$$H^{AS} = \begin{cases} 1 & \text{if } \left\{\frac{{R_s}^{AS} < F < {R_f}^{AS}}{\dot{F}>0}\right. \\ 0 & \text{otherwise} \end{cases} \tag{7}$$

$$H^{SA} = \begin{cases} 1 & \text{if } \left\{\frac{{R_f}^{SA} < F < {R_s}^{SA}}{\dot{F}<0}\right. \\ 0 & \text{otherwise} \end{cases} \tag{8}$$

where ${R_s}^{AS} = {\sigma_s}^{SA}(1+\alpha)$.

ISSN 2176-5480

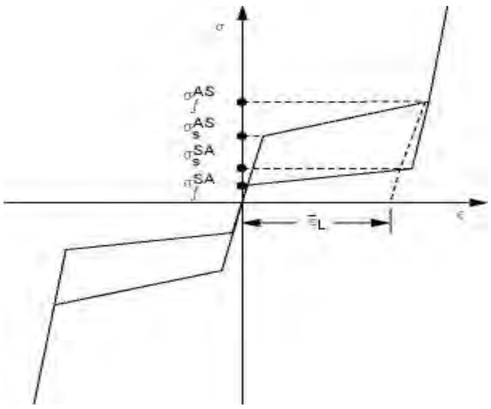

Figure 1. Idealized stress-strain diagram of superelastic behavior of SMA (ANSYS, 2013).

The parameter α characterizes the tension-compression asymmetry. In case of symmetric behavior, $\alpha = 0$. For a uniaxial tension-compression test, α can be related to the initial value of austenite to martensite phase transformation in tension and compression (${\sigma_c}^{AS}$ and ${\sigma_t}^{AS}$, respectively) as defined by Eq. (9):

$$\alpha = \frac{{\sigma_c}^{AS} - {\sigma_t}^{AS}}{{\sigma_c}^{AS} + {\sigma_t}^{AS}} \tag{9}$$

The stress-strain relation is defined by Eqs. (10) and (11):

$$\sigma = \mathbf{D} : (\varepsilon - \varepsilon_{tr}) \tag{10}$$

$$\dot{\boldsymbol{\varepsilon}}_{tr} = \dot{\beta}\, \bar{\boldsymbol{\varepsilon}}_L \frac{\partial F}{\partial \sigma} \tag{11}$$

where $\mathbf{D}$ is the elastic stiffness tensor, $\boldsymbol{\varepsilon}_{tr}$ is the transformation strain tensor, and $\bar{\boldsymbol{\varepsilon}}_L$ is the material parameter. The material parameters for the superelastic SMA model are defined in Tab. (1).

Table 1. Constitutive parameters for superelastic behavior in SMA.

Parameter	**Property**
${\sigma_s}^{AS}$ (MPa)	Starting stress value for the forward (austenite – martensite) phase transformation
${\sigma_f}^{AS}$ (MPa)	Final stress value for the forward (austenite – martensite) phase transformation
${\sigma_s}^{SA}$ (MPa)	Starting stress value for the reverse (martensite – austenite) phase transformation
${\sigma_f}^{SA}$ (MPa)	Final stress value for the reverse (martensite – austenite) phase transformation
$\bar{\boldsymbol{\varepsilon}}_L$	Maximum transformation strain
α	Parameter measuring the difference between material responses in tension and compression

Lima *et al.* (2011) defined constitutive parameters from experimental tension test by considering superelastic Ni-Ti orthodontic wire. Table (2) regarding the temperatures $T = 30$°C, $T = 65$°C and $T = 75$°C. These values are employed for numerical simulations, and should be employed to interpolate values in order to develop analysis for other temperatures.

Table 2. Thermomechanical properties of the Ni-Ti SMA (Lima *et al.*, 2011).

Parameters / Temperature	$\boldsymbol{T = 30}$°C	$\boldsymbol{T = 65}$°C	$\boldsymbol{T = 75}$°C
${\sigma_s}^{AS}$ (MPa)	199	351.51	407.51
${\sigma_f}^{AS}$ (MPa)	320	440.13	504.13
${\sigma_s}^{SA}$ (MPa)	195	366	425
${\sigma_f}^{SA}$ (MPa)	70.44	189.24	223.24
$\bar{\boldsymbol{\varepsilon}}_L$	0.033	0.032	0.03
α	0	0	0
E (GPa)	22	23	25.45
μ	0.3	0.3	0.3

ISSN 2176-5480

2.2 Analytical model to calculate the force-displacement behavior in conical washers

Almen and László (1936) developed a theory for the calculations of conical washers with linear materials assuming that a spring flank rotates around a center of rotation during deflection. Figure (2) presents a schematic picture of the device and the center of rotation is defined by the diameter D_0, expressed by Eq. (12).

$$D_0 = \frac{D_e - D_i}{\ln\left(\frac{D_e}{D_i}\right)} \tag{12}$$

where D_e and D_i is the outer and inner diameters, respectively, as shown in Fig. (2).

The calculations assume that material behavior remains linear during loading, the washer cross-section is rectangular with sharp corners and the washer remains in one plane during deflection. The load is applied at points I and III, as defined in the model of Fig. (2).

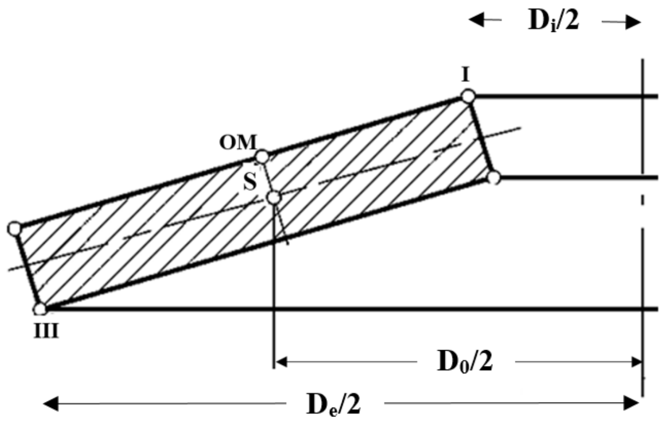

Figure 2. Half section of a conical Belleville washer with definition of position of the center of rotation, point OM and characteristic radius.

Equation (13) establishes an analytical force-displacement relationship for conical washers manufactured with linear materials.

$$F = \frac{4E}{1-\mu^2}\frac{t^4}{K_1 {D_e}^2}\frac{s}{t}\left[\left(\frac{h}{t}-\frac{s}{t}\right)\left(\frac{h}{t}-\frac{s}{2t}\right)+1\right] \tag{13}$$

The constants δ and K_1 for the analytical model can be obtained by Eqs. (14) and (15).

$$\delta = \frac{D_e}{D_i} \tag{14}$$

$$K_1 = \frac{1}{\pi}\frac{\left(\frac{\delta-1}{\delta}\right)^2}{\frac{\delta+1}{\delta-1}-\frac{2}{ln\delta}} \tag{15}$$

The geometrical parameters for the analytical model are defined in Tab. (3).

ISSN 2176-5480

Table 3. Parameters for the analytical model described by Eq. (13).

Symbols	Designation
δ	Diameter ratio
D_e	Outside diameter
D_i	Inside diameter
K_1	Constant
F	Applied force of a single washer
E	Young's modulus
μ	Poisson ratio
s	Deflection of a single washer
t	Thickness
h	Cone height of an unloaded single washer

2.3 FEM model for conical washers

The Finite Element Method (FEM) analysis for the SMA superelastic conical washers is carried out using ANSYS®. Basically, a two-dimensional axisymmetric element (PLANE 183) is employed considering axisymmetric situations. This element has 8 nodes with 2 degrees of freedom each. Figure (3) shows a picture of the FEM model.

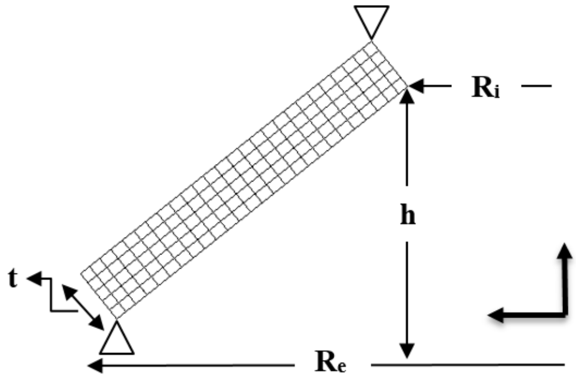

Figure 3. Axisymmetric FEM model and mesh for simulation of the force vs. deflection behavior of SMA superelastic Belleville washers.

A convergence analysis was performed by considering force-displacement curves. Figure (4) shows several results obtained with different elements. Note that Ni-Ti SMA Belleville washer with h/t = 8 and R_e/R_i = 1.5 at T = 30 ºC are considered. It is important to observe the strong nonlinearity represented by the hysteretic behavior that we called duckbill response. The evaluation of the optimal number of elements was performed by checking the variation in results with different configurations of meshes. Based on these results, it is assumed a mesh with at least 234 elements. It was verified that higher number of elements and the 234 present similar results.

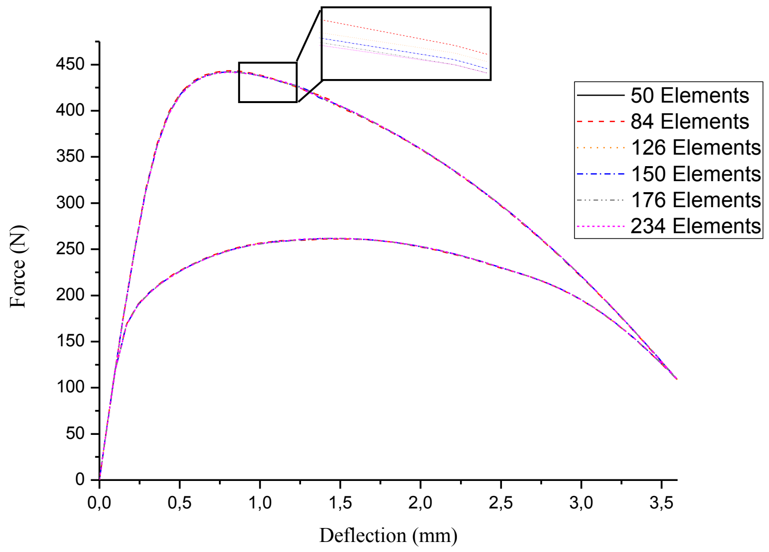

Figure 4. Convergence test for 2D axisymmetric FEM model.

Another way to verify the capability of the FEM model to describe the thermomechanical behavior of the SMA washer is to establish a comparison with the analytical model discussed in section 2.2 for elastic washers. Figure (5) presents this comparison showing a qualitative good agreement. Note that SMA washer has a hysteretic behavior during loading and unloading due to the reversible phase transformation from austenite to stress induced martensite. The elastic analytical model contemplates no hysteresis, so that the numerical model is more realistic.

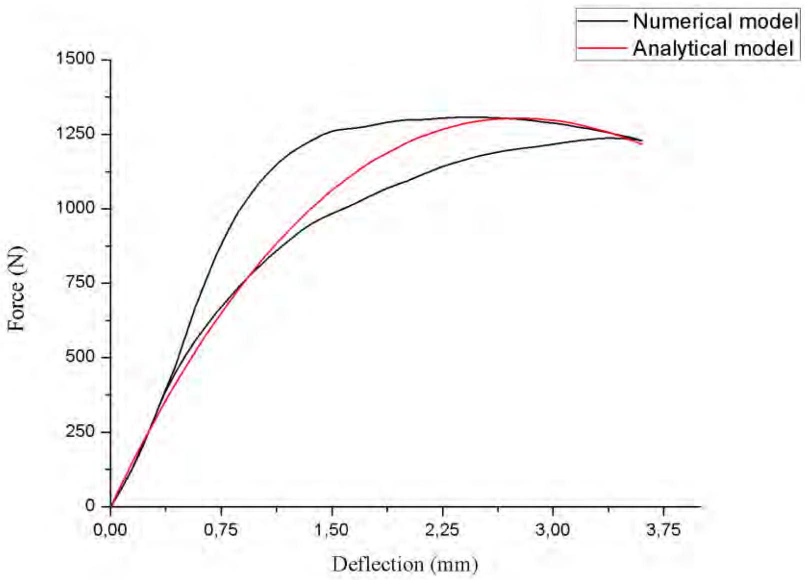

Figure 5. Comparison between the 2D non-linear FEM model (SMA) and analytical elastic model.

3. RESULTS AND DISCUSSIONS

Different geometric configurations are evaluated based on dimensionless parameters. Basically, two geometrical aspects are investigated: h/t and R_e/R_i. Moreover, different temperatures are investigated. Figure (6) shows force-displacement simulated curves for $h/t = 8$ and $R_e/R_i = 1.5$ at three different temperatures defined in Tab. (3): 30°C, 65°C and 75°C. Note that curves present a hysteretic behavior characterized by the duckbill pattern.

There are few experimental results for force-displacement curves of SMA Belleville washers in the literature (Labrecque *et al.*, 1996; Speicher *et al.*, 2009; Speicher, 2010). Figure (7) presents experimental force-displacement curves due to Speicher *et al.* (2009) allowing a qualitative comparison with numerical simulations. Note the same duckbill pattern. The difference between the force range in the results of the force-displacement curves showed in Figs.

ISSN 2176-5480

(6) and (7) are due to the difference in the geometrical parameters of the numerical (Fig. 6) and experimental case from literature (Fig. 7), as cone height of an unloaded single washer *(h)*, thickness *(t)*, outside radius (R_e) and inside radius (R_i).

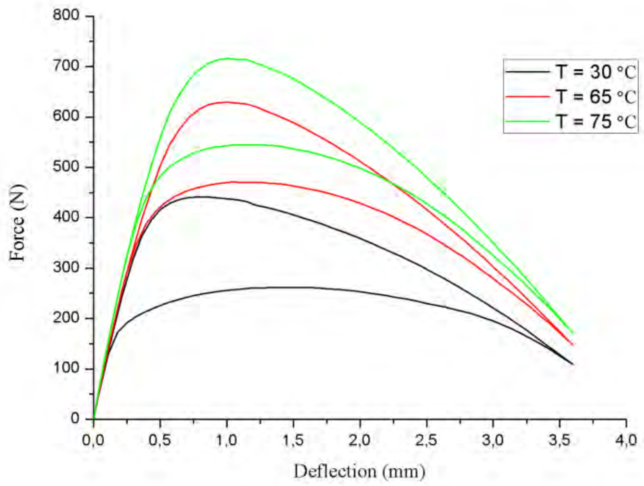

Figure 6. Duckbill macro mechanical phenomenon in a Belleville SMA washer simulated with the 2D FEM model.

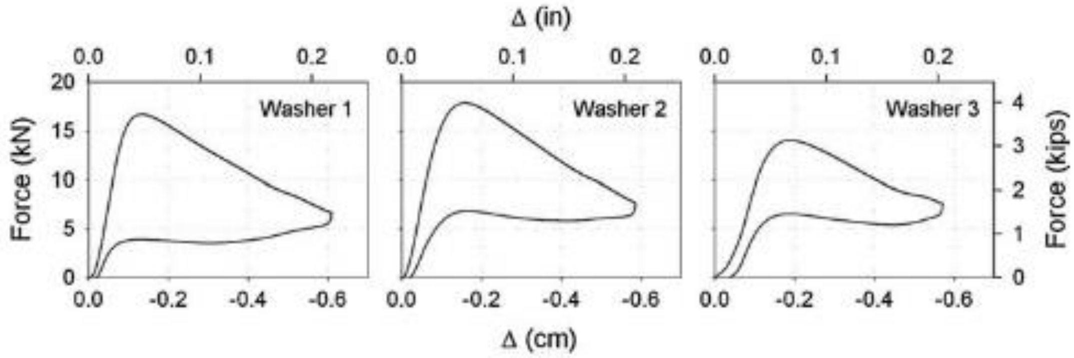

Figure 7. Experimental force-displacement behavior of Ni-Ti SMA Belleville washers obtained by Speicher *et al.* (2009).

Force-displacement curves for several temperatures are constructed by considering interpolation of constitutive parameters for several temperatures. Two different geometric aspects are of concern. Figure (8) presents h/t = 4 and R_e/R_i = 2.5 while Fig. (9) shows h/t = 4 and R_e/R_i = 1.5. Note the temperature dependent behavior associated with the duckbill pattern.

ISSN 2176-5480

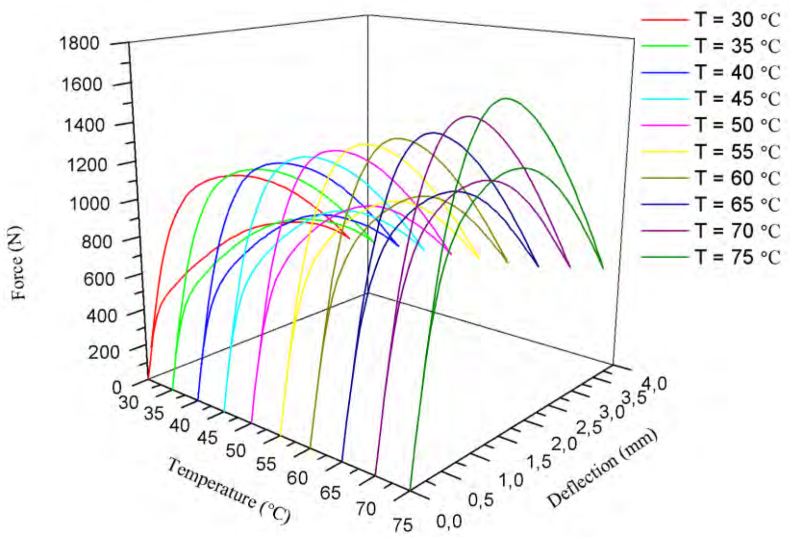

Figure 8. Force-displacement curves of a SMA Belleville washer with $h/t = 4$ and $R_e/R_i = 2.5$ for interpolated temperatures with 2D FEM model.

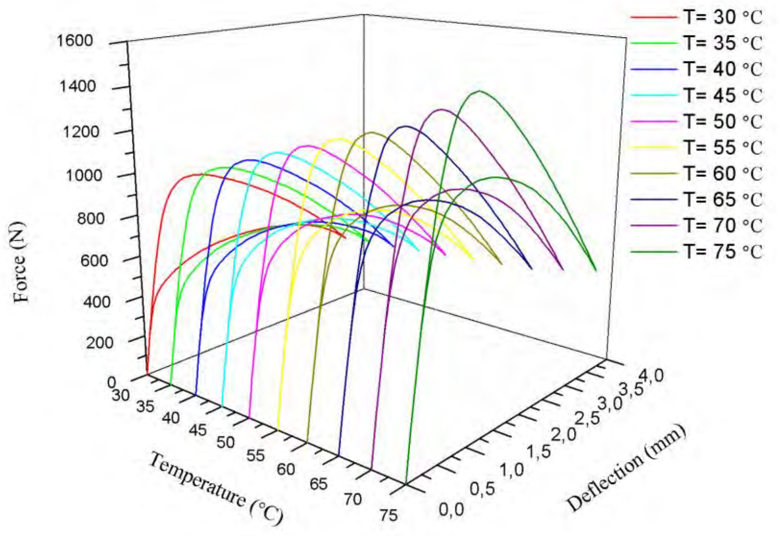

Figure 9. Force-displacement curves of a SMA Belleville washer with $h/t = 4$ and $R_e/R_i = 1.5$ for interpolated temperatures with 2D FEM model.

4. CONCLUSIONS

This paper deals with a preliminary numerical analysis of the force-displacement behavior of Ni-Ti SMA washers using the finite element method. It is demonstrated that a 2D axisymmetric FEM model is sufficient to capture the general thermomechanical characteristic of these conical SMA washers. Geometric aspects are investigated by varying dimensionless parameters (h/t and R_e/R_i). Numerical simulations present results in qualitative agreement with experimental data available in literature. The superelastic nonlinear force-displacement behavior of Ni-Ti SMA Belleville washers has a duckbill pattern characterized by a hysteretic behavior. Temperature dependence of the SMA washer is analyzed showing the classical SMA behavior where the increase of temperature induces higher forces necessary to produce the same displacement in the nonlinear path.

ISSN 2176-5480

5. ACKNOWLEDGEMENTS

The authors thank the CNPq Brazilian Agency for funding the following research projects: INCT of Smart Structures for Engineering (Project 574001/2008-5), Casadinho UFCG-UFRJ-ITA (Project 552199/2011-7), Universal 14/2011 (Project 472771/2011-6), PQ 2 (Project 302320/2011-3) and PQ 1B (Project 300723/2009-1). The support of FAPERJ and AFOSR are also acknowledged.

6. REFERENCES

Almen J. O., Laszlo A., 1936. The uniform–section disk spring. Transactions of ASME, pp. 305 - 315.

ANSYS user's manual Version 14.5. ANSYS Inc. 2013.

Auricchio, F., 2001. A Robust Integration-Algorithm for a Finite-Strain Shape-Memory-Alloy Superelastic Model. International Journal of Plasticity, Vol. 17, pp. 971–990.

Auricchio, F., Taylor, R. L., Lubliner., J., 1997. Shape-Memory Alloys: Macromodeling and Numerical Simulations of the Superelastic Behavior. Computational Methods in Applied Mechanical Engineering, 146:281–312..

Lagoudas, D. C., 2008. Shape Memory Alloys: Modeling and Engineering Applications. Texas: Springer

Labrecque, C., Braunovic, M., Terriault, P., Trochu, F. and Schetky, M., 1996. Experimental and Theoretical Evaluation of the Behavior of a Shape Memory Alloy Belleville Washer under Different Operating Conditions. 42nd IEEE Holm Conference on Electrical Contacts Joint with the 18th International Conference on Electrical Contacts, Chicago, USA.

Lima, I. S. T., Simões, J. B., De Araújo, C. J., Santos, N. C., 2011. Numerical and Experimental Analysis of the Superelastic Behavior of a Ni-Ti Orthodontic Wire. In: 21st Brazilian Congress of Mechanical Engineering (COBEM), Proceedings of COBEM 2011, Natal – RN, Brazil, pp. 1 - 9.

Otsuka, K., Wayman, C.M., 1998. Shape Memory Materials. Edited by K. Otsuka and C. M. Wayman, Cambridge University Press, Cambridge, England.

Pereira, F. F. R., Simões, J. B., Reis, R. P. B., De Araújo, C. J., 2011. Thermomechanical Tests of Shape Memory Alloy Belleville Washers. In: 21st Brazilian Congress of Mechanical Engineering (COBEM), Proceedings of COBEM 2011, Natal – RN, Brazil, pp. 1 - 10.

Simões, J. B., 2012. Thermomechanical Characterization of Belleville Actuators of Shape Memory Alloys. M.Sc Thesis: Mechanical Engineering Department, Federal University of Campina Grande, Campina Grande - PB, Brazil, 116p.

Speicher M., 2010. Cyclic Testing and Assessment of Shape Memory Alloy recentering systems. Thesis (Doctor) - Philosophy in the School of Civiland Environmental Engineering, Georgia Institute of Technology, EUA.

Speicher M., Hodgson D. E., Desroches R. and Leon R. T., 2009. Shape Memory Alloy Tension/Compression Device for Seismic Retrofit of Buildings. Journal of Materials Engineering and Performance, Vol. 18, pp.746–753.

7. RESPONSIBILITY NOTICE

The authors are the only responsible for the printed material included in this paper.